# Vibrational spectroscopy of the borate mineral chambersite MnB$_7$O$_{13}$Cl – Implications for the molecular structure

Ray L. Frost [a,*], Andrés López [a], Ricardo Scholz [b], Yunfei Xi [a]

[a] School of Chemistry, Physics and Mechanical Engineering, Science and Engineering Faculty, Queensland University of Technology, GPO Box 2434, Brisbane, Queensland 4001, Australia
[b] Geology Department, School of Mines, Federal University of Ouro Preto, Campus Morro do Cruzeiro, Ouro Preto, MG 35,400-00, Brazil

HIGHLIGHTS

- Chambersite is a manganese borate mineral MnB$_7$O$_{13}$Cl.
- It occurs as colorless crystals in the monoclinic pyramidal crystal system.
- Chambersite is related to boracite and shows ferroelectric properties.
- Vibrational spectroscopy characterises the mineral.

GRAPHICAL ABSTRACT
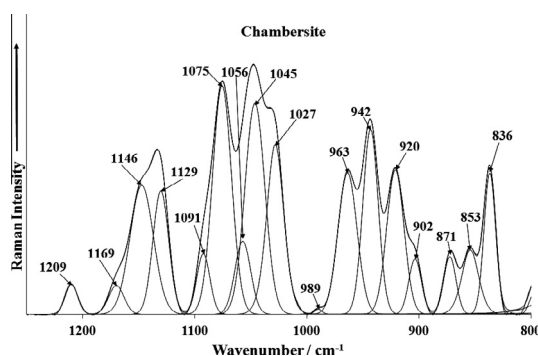
ABSTRACT

Chambersite is a manganese borate mineral with formula: MnB$_7$O$_{13}$Cl and occurs as colorless crystals in the monoclinic pyramidal crystal system. Raman bands at 902, 920, 942 and 963 cm^{-1} are assigned to the BO stretching vibration of the B$_7$O$_{13}$ units. Raman bands at 1027, 1045, 1056, 1075 and 1091 cm^{-1} are attributed to the BCl in-plane bending modes. The intense infrared band at 866 cm^{-1} is assigned to the trigonal borate stretching modes. The Raman band at 660 cm^{-1} together with bands at 597, 642 679, 705 and 721 cm^{-1} are assigned to the trigonal and tetrahedral borate bending modes. The molecular structure of a natural chambersite has been assessed using vibrational spectroscopy.

© 2013 Elsevier B.V. All rights reserved.

Introduction

Chambersite is a manganese borate mineral formula Mn$_3$B$_7$O$_{13}$Cl [1]. The mineral is a member of the borate mineral series that includes ericaite and boracite. Chambersite is the manganese analogue of boracite. It was first discovered at Barber's Hill salt dome, Chambers County, Texas, USA. The mineral is also known from the Dongshuichang deposits in Jixan, Tianjin, China [2]. The mineral is an evaporite mineral and occurs associated with other evaporite minerals such as halite, anhydrite and gypsum. The mineral is known for a number of significant borate deposits worldwide [3–6]. It occurs in brine residues from extraction wells in salt domes.

Boracite is a magnesium borate mineral with formula: Mg$_3$B$_7$O$_{13}$Cl [7] and occurs as blue green, colorless, gray, yellow to white crystals in the orthorhombic–pyramidal crystal system [8,9]. Bora-

* Corresponding author. Tel.: +61 7 3138 2407; fax: +61 7 3138 1804.
   E-mail address: r.frost@qut.edu.au (R.L. Frost).

cite also shows pseudo-isometric cubical and octahedral forms [10]. These are thought to be the result of transition from an unstable high temperature isometric form upon cooling. The mineral is related to the homonymous group that includes chambersite – $(Mn^{2+})_3B_7O_{13}Cl$, congolite – $(Fe^{2+},Mg)_3B_7O_{13}Cl$, ericaite – $(Fe^{2+})_3B_7O_{13}Cl$ and trembathite – $(Mg,Fe^{2+})_3B_7O_{13}Cl$. Boracite is typically found in evaporite sequences associated with gypsum, anhydrite, halite, sylvite, carnallite, kainite and hilgardite.

The mineral chambersite has been synthesised [11–13]. The reason for the synthetic analogues of chambersite is the ferroelectric properties of the mineral. Chambersite is orthorhombic, pseudocubic. Crystals are pseudotetrahedral. The cell data is: *Space Group: Pca*21 with *a* = 8.68(1), *b* = 8.68(1), *c* = 12.26(1) and *Z* = 4. Boracite is orthorhombic, pseudocubic of point group: mm^2 [14] and space group: *Pca2₁*, with unit-cell parameters *a* = 8.577(6), *b* = 8.553(8), *c* = 12.09(1) and *Z* = 4 [9,14–16]. Boracite is dimorphic with trigonal trembathite $(Mg,Fe)_3(B_7O_{13})Cl$ and forms a series with ericaite $Fe_3^{2+}(B_7O_{13})Cl$ (named after English heather because of the reddish color). The boracite group mineral congolite has a trigonal structure [10]; however the higher temperature form is cubic with a phase transition temperature of 268 °C [17,18].

The number of vibrational spectroscopic studies of borate minerals is quite few and far between [19–22]. The number of Raman studies of borate minerals is also very limited [23,24]. There have been a number of infrared studies of some natural borates [25–28]. Most of these references are not new and there have been no recent studies on the vibrational spectroscopy of natural borates. Ross in Farmer's treatise reported the infrared spectra of several borate minerals [29]. The use of infrared spectroscopy is limited by the spatial resolution of the technique which is around 25 microns. In comparison, the spatial resolution using Raman spectroscopy is 1 μm. Thus, when studying a mineral using spectroscopic techniques it is advantageous to use Raman spectroscopy. The selection of the target mineral is more easily made. With infrared spectroscopy, any impurities will be measured as well as the target mineral. Raman spectroscopy has proven most useful for the study of secondary minerals.

To the best of the authors' knowledge, there have been very few infrared spectroscopic studies of chambersite type structure [28,30] and few Raman studies of this natural mineral have been forthcoming. What Raman studies that have been undertaken are related to the determination of the ferroelectric transition point. Thermodynamic studies of this transition have been forthcoming [31]. In this way the cubic (43 m) → orthorhombic (mm^2) ferroelectric phase transition is determined. Burns showed the application of powder diffractions to identify boracites [32]. The structure of boracites has been refined [10]. A wide range of boracites have been synthesised and their dielectric properties determined [33]. The effect of the metal cations and halogens on the B–O bonds in the boracite structure was studied by IR spectroscopy [34]. Many of the boracites show ferroelectric properties [35] and some Raman studies have been undertaken to determine the ferroelectric phase transitions [36–38]. Vibrational spectroscopy has focussed on the ferroelectric transitions. Different types of boracites have been synthesised.

The objective of this paper is to report the vibrational spectroscopic study of a natural chambersite mineral and relate the spectra to the molecular chemistry and the crystal chemistry of this borate mineral. We have characterised chambersite using a combination of Raman and infrared spectroscopy.

Experimental

Mineral

The sample of chambersite was incorporated into the collection of the Geology Department of the Federal University of Ouro Preto,
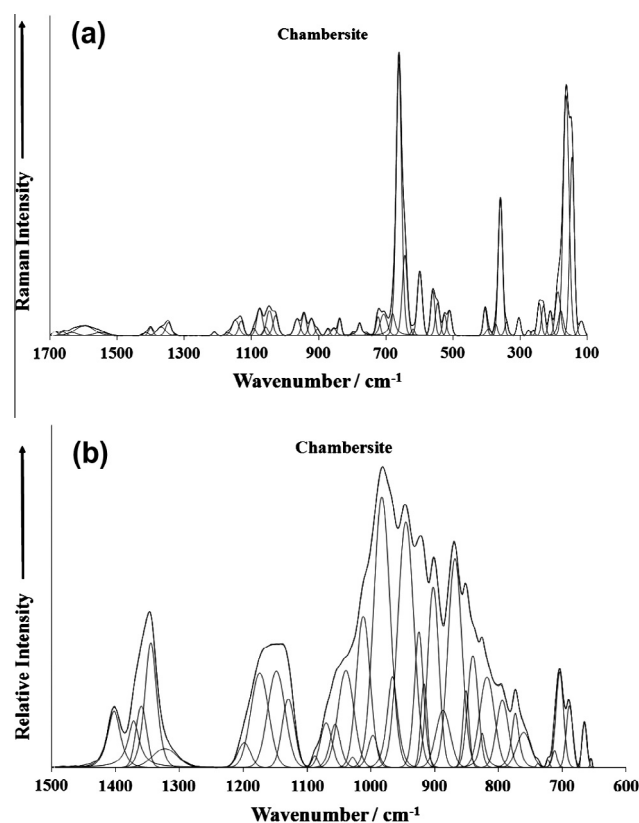

Fig. 1. (a) Raman spectrum of chambersite (upper spectrum) over the 100 to 1700 cm^{-1} spectral range and (b) infrared spectrum of chambersite (lower spectrum) over the 600 to 1500 cm^{-1} spectral range.

Minas Gerais, Brazil, with sample code SAC-114. The sample was gently crushed and the associated minerals were removed under a stereomicroscope Leica MZ4. Scanning electron microscopy (SEM) was applied to support the chemical characterization. Details of the mineral have been published (page 80, vol. 5) [39].

Raman spectroscopy

Crystals of chambersite were placed on a polished metal surface on the stage of an Olympus BHSM microscope, which is equipped with 10×, 20×, and 50× objectives. The microscope is part of a Renishaw 1000 Raman microscope system, which also includes a monochromator, a filter system and a CCD detector (1024 pixels). The Raman spectra were excited by a Spectra-Physics model 127 He–Ne laser producing highly polarised light at 633 nm and collected at a nominal resolution of 2 cm^{-1} and a precision of ± 1 cm^{-1} in the range between 200 and 4000 cm^{-1}. Repeated acquisitions on the crystals using the highest magnification (50×) were accumulated to improve the signal to noise ratio of the spectra. The spectra were collected over night. Raman Spectra were calibrated using the 520.5 cm^{-1} line of a silicon wafer. The Raman spectrum of at least 10 crystals was collected to ensure the consistency of the spectra.

Infrared spectroscopy

Infrared spectra were obtained using a Nicolet Nexus 870 FTIR spectrometer with a smart endurance single bounce diamond ATR cell. Spectra over the 4000–525 cm^{-1} range were obtained by the co-addition of 128 scans with a resolution of 4 cm^{-1} and a

mirror velocity of 0.6329 cm/s. Spectra were co-added to improve the signal to noise ratio.

Spectral manipulation such as baseline correction/adjustment and smoothing were performed using the Spectracalc software package GRAMS (Galactic Industries Corporation, NH, USA). Band component analysis was undertaken using the Jandel 'Peakfit' software package that enabled the type of fitting function to be selected and allows specific parameters to be fixed or varied accordingly. Band fitting was done using a Lorentzian–Gaussian cross-product function with the minimum number of component bands used for the fitting process. The Lorentzian–Gaussian ratio was maintained at values greater than 0.7 and fitting was undertaken until reproducible results were obtained with squared correlations of r^2 greater than 0.995.

Results and discussion

The Raman spectrum of chambersite in the 100 to 1700 cm^{-1} region is displayed in Fig. 1a. This figure reports the position of the Raman bands and their relative intensity. It is noted that there are parts of the spectrum where little intensity is observed. Therefore, the spectrum is subdivided into sections in subsequent figures so that more detailed assessment of the spectrum can be made. It is noted that no intensity is observed above 1700 cm^{-1}. In a similar way, the infrared spectrum of chambersite in the 600 to 1500 cm^{-1} region is reported in Fig. 1b. It should be noted no intensity was observed above 1500 cm^{-1}. The spectrum is not shown below 600 cm^{-1}. The reason for this is that we are using a reflectance technique and the ATR cell absorbs all incident radiation. In a similar fashion to the Raman spectrum, the infrared spec-

trum is divided into sections depending upon the types of vibrations being observed.

The Raman spectrum of chambersite in the 800 to 1300 cm^{-1} spectral range is reported in Fig. 2a. The infrared spectrum of chambersite in the 650 to 900 cm^{-1} spectral range is reported in Fig. 2b. The Raman spectrum in this spectral region is noted for the large number of bands with groups of bands observed. The first group of bands is between 800 and 900 cm^{-1}. The second group lies between 900 and 1000 cm^{-1}. The third group is found between 1000 and 1100 cm^{-1}. The fourth group is between 1100 and 1300 cm^{-1}. The second grouping with Raman bands at 902, 920, 942 and 963 cm^{-1} are assigned to the BO stretching vibration of the B_7O_{13} units. The Raman bands at 1027, 1045, 1056, 1075 and 1091 cm^{-1} are attributed to the BCl in-plane bending modes. Iliev et al. determined the Raman spectrum of a synthetic cobalt chambersite [37]. The symmetry species of some vibrational modes were determined. Iliev et al. [40] used Raman imaging to show the ferroelectric properties of chambersite type compounds. These workers [40] showed that chambersites exhibit a sequence of transitions from the high temperature paraelectric cubic phase to ferroelectric orthorhombic, monoclinic, trigonal phases, and finally to a monoclinic phase at low temperatures where both ferroelectric and magnetic orders coexist. Kim and Somoano determined the improper ferroelectric transition using Raman spectroscopy [38].

In contrast, the infrared spectrum of chambersite (Fig. 2b) shows complexity with many overlapping bands, making the assignment of the infrared bands very difficult. The intense infrared band at 866 cm^{-1} with other infrared bands at 771, 792, 816, 823, 838 and 849 cm^{-1} is assigned to the trigonal borate stretching modes. The overlapping infrared bands at 771, 792, 816, 823, 838
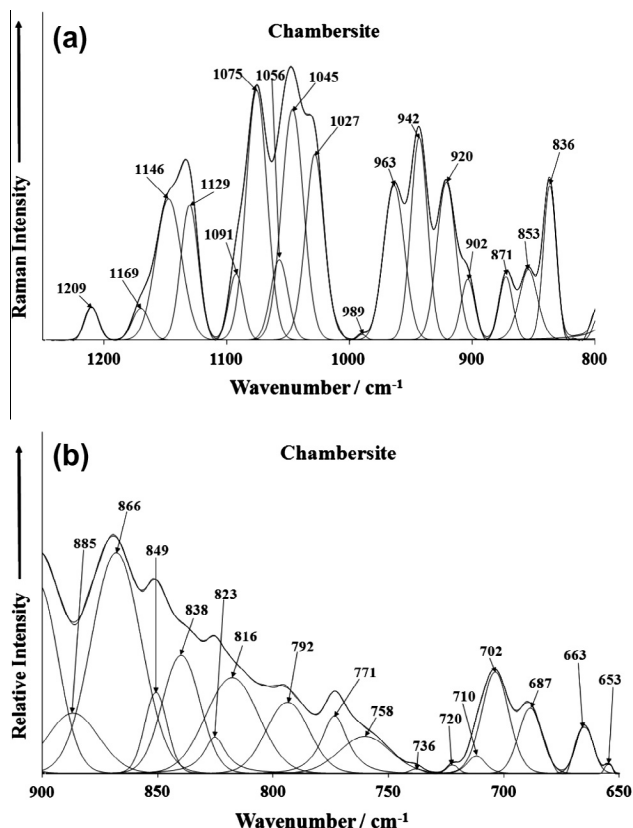

Fig. 2. (a) Raman spectrum of chambersite over the 800 to 1300 cm^{-1} spectral range 2 and (b) infrared spectrum of chambersite over the 650 to 900 cm^{-1} spectral range.
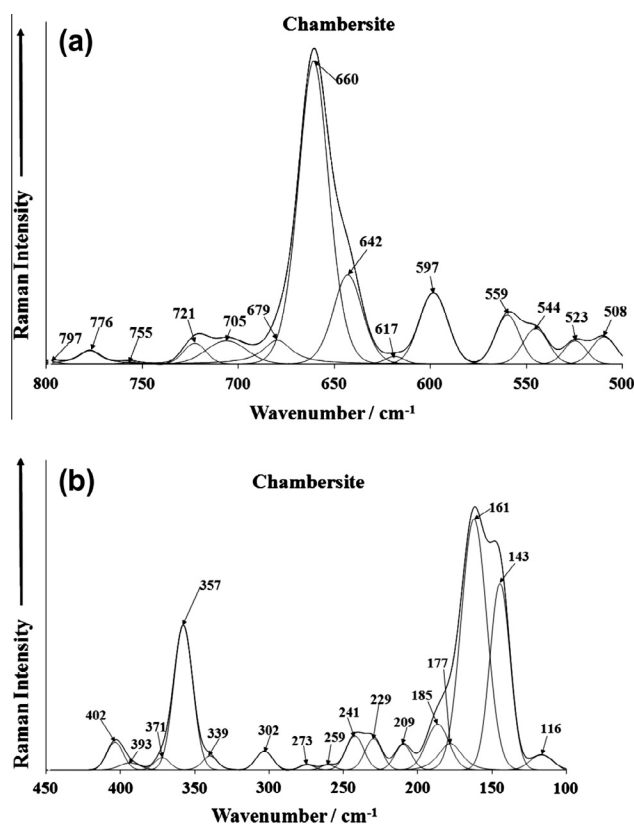

Fig. 3. (a) A Raman spectrum of chambersite (upper spectrum) in the 500 to 800 cm^{-1} spectral range and (b) infrared spectrum of chambersite (lower spectrum) in the 100 to 450 cm^{-1} spectral range.
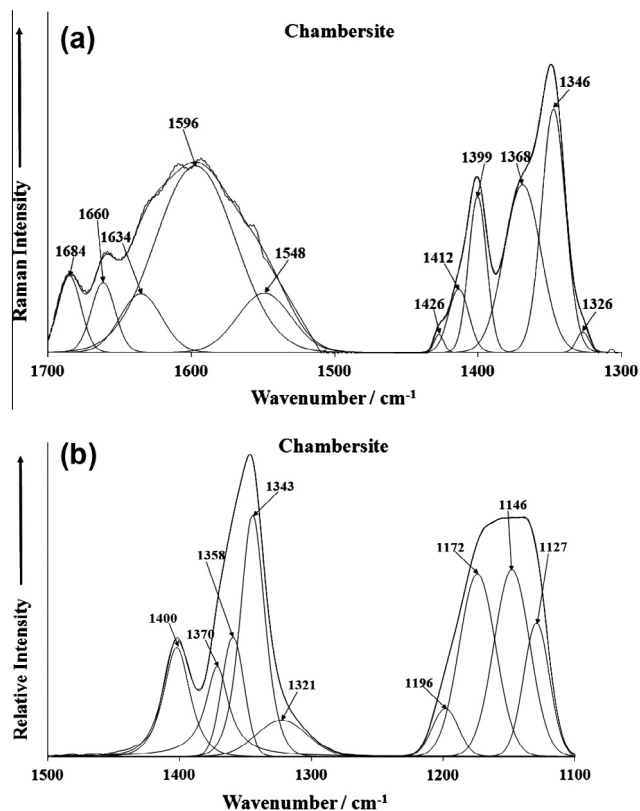
Fig. 4. (a) Raman spectrum of chambersite (upper spectrum) in the 1300 to 1700 cm^{-1} spectral range and (b) infrared spectrum of chambersite (lower spectrum) in the 1100 to 1500 cm^{-1} spectral range.

and 849 cm^{-1} are attributed to the infrared tetrahedral borate stretching and bending vibrations. The series of bands from 650 through to 720 cm^{-1} are related to trigonal borate bending modes.

The Raman spectra in the 500 to 800 cm^{-1} and in the 100 to 450 cm^{-1} spectral range are illustrated in Fig. 3a and b. The spectrum in Fig. 3a is dominated by an intense Raman band at 660 cm^{-1}. Other low intensity bands are found at 597, 642 679, 705 and 721 cm^{-1}. These bands are simply defined as trigonal and tetrahedral borate bending modes. A series of infrared bands at 653, 663, 687, 702, 710 and 720 cm^{-1} are due to these bending modes. Strong Raman bands are found in the far wavenumber region at 143, 161 and 357 cm^{-1} (Fig. 3b). These bands may be simply described as lattice vibrations.

The development of these types of compounds such as chambersite rests with their ferromagnetic and pyro-electric properties [41]. The development of piezoelectric properties is time continuous [42,43]. Also a hydroxy compound has been synthesised [44], although the vibrational spectroscopy of this compound was not reported. In the infrared spectrum (Fig. 3b) a series of low intensity bands are observed (see Fig. 4).

Conclusions

There are many borate minerals which have yet to have their vibrational spectrum determined and the molecular structure assessed in terms of their vibrational spectrum. In this work we have measured the Raman and infrared spectrum of chambersite, a halogenated borate mineral of manganese with formula Mn$_3$B$_7$O$_{13}$Cl. The importance of the mineral chambersite rests with the chemistry of the compound and the range of isomorphic substitutions which can be made in order to produce specially selected ferroelectric, pyroelectric and piezoelectric properties.

References

[1] R.M. Honea, F.R. Beck, Am. Mineral. 47 (1962) 665–671.
[2] D. Fan, P. Yang, R. Wang, Ore Geol. Rev. 15 (1999) 15–29.
[3] P.M. Bilonizhka, O.N. Vynar, V.S. Mel'nikov, P.K. Vovk, Vopr. Mineral. Osad. Obraz. 8 (1970) 80–88.
[4] P.M. Bilonizhka, O.N. Vynar, V.S. Mel'nikov, P.K. Vovk, Doklady 191 (1970) 1127–1129.
[5] V.N. Dubinina, Trudy Vsesoyuznogo Nauchno-Issledovatel'skogo Instituta Galurgii 54 (1969) 193–208.
[6] J.D. Grice, R.A. Gault, J. Van Velthuizen, Can. Mineral. 43 (2005) 1469–1487.
[7] J.W. Gruner, Am. Mineral. 13 (1928) 481–483.
[8] J.W. Gruner, Am. J. Sci. 17 (1929) 453–460.
[9] T. Ito, N. Morimoto, R. Sadanaga, Acta Cryst. 4 (1951) 310–316.
[10] E. Dowty, J.R. Clark, Z. Kristallogr. 138 (1973) 64–99.
[11] J.C. Joubert, J. Muller, M. Pernet, B. Ferrand, Bull. Soc. Fr. Mineral. 95 (1972) 68–74.
[12] Y. Zeng, Dizhi Xuebao 57 (1983) 401–409.
[13] Y. Zeng, J.G. Liou, Neues Jahr. Mineral. (1982) 69–83.
[14] G. Berset, W. Depmeier, R. Boutellier, H. Schmid, Acta Cryst. C41 (1985) 1694–1696.
[15] M. Mehmel, Fortschr. Mineral. Kristallogr. Petrog. 17 (1932) 436–437.
[16] R.J. Nelmes, J. Phys. C7 (1974) 3840–3854.
[17] P.C. Burns, M.A. Carpenter, Can. Mineral. 34 (1996) 881–892.
[18] S. Sueno, J.R. Clark, J.J. Papike, J.A. Konnert, Am. Mineral. 58 (1973) 691–697.
[19] M. Mir, J. Janczak, Y.P. Mascarenhas, J. Appl. Cryst. 39 (2006) 42–45.
[20] I. Mitov, Z. Cherkezova-Zheleva, V. Mitrov, J. Balkan Trib. Ass. 4 (1998) 191–200.
[21] A.S. Povarennykh, E.I. Nefedov, Geol. Zh. 31 (1971) 13–27.
[22] V.S. Suknev, E.N. Diman, Zh. Prikladnoi Spektros. 10 (1969) 326–328.
[23] V.F. Ross, J.O. Edwards, Chem. Boron Compd. (1967) 15–207.
[24] R.L. Frost, J. Raman Spectrosc. 42 (2011) 540–543.
[25] M.V. Akhmanova, Zh. Strukt. Khim. 3 (1962) 28–34.
[26] D.A. Long, R.T. Bailey, Spectrochim. Acta 19 (1963) 1607–1610.
[27] A. Vasko, I. Srb, Czech. J. Phys. 17 (1967) 1110–1123.
[28] C.E. Weir, J. Res. Nat. Bur. Standards A70 (1966) 153–164.
[29] V.C. Farmer, Mineralogical Society Monograph 4: The Infrared Spectra of Minerals, London, 1974.
[30] C. Helvaci, Mercian Geol. 6 (1978) 257–270.
[31] A. Guillermo Castellanos-Guzman, J. Solid State Chem. 54 (1984) 78–83.
[32] P.C. Burns, Powder Diff. 10 (1995) 250–260.
[33] F. Jona, J. Phys. Chem. 63 (1959) 1750–1752.
[34] V.I. Bugakov, V.P. Orlovskii, T.V. Belyaevskaya, Y.A. Bobrov, V.L. Egorov, N.N. Morozov, V.I. Pakhomov, Izvestiya Akad. Nauk SSSR 15 (1979) 1037–1041.
[35] J. Campa-Molina, S. Ulloa-Godinez, A. Barrera, L. Bucio, J. Mata, J. Phys. 18 (2006) 4827–4837.
[36] D.J. Lockwood, Ferroelectrics 13 (1976) 353–354.
[37] M.N. Iliev, V.G. Hadjiev, M.E. Mendoza, J. Pascual, Phys. Rev. B 76 (2007). 214112/214111–214112/214115.
[38] Q. Kim, R.B. Somoano, Ferroelectrics 36 (1981) 431–434.
[39] J.W. Anthony, R.A. Bideaux, K.W. Bladh, M.C. Nichols, Silica, Silicates, Mineral data Publishing, Tucson, Arizona, 1995.
[40] M.N. Iliev, V.G. Hadjiev, J. Iniguez, J. Pascual, Acta Phys. Pol. A116 (2009) 19–24.
[41] A.G. Castellanos-Guzman, 200 years of research on boracites, ISAF '94, Proceedings of the IEEE International Symposia Applied Ferroelectrics, 9th University Park, Pa, Aug. 7–10, 1994, 6–9.
[42] O. Crottaz, J.P. Rivera, H. Schmid, J. Korean Phys. Soc. 32 (1998) S1261–S1264.
[43] M. Delfino, G.M. Loiacono, P.S. Gentile, Inorg. Chim. Acta 43 (1980) 59–63.
[44] U. Werthmann, H. Gies, J. Glinnemann, T. Hahn, Zeit. Kristallogr. 215 (2000) 393–396.